Available online at www.sciencedirect.com

ScienceDirect

Scripta Materialia 61 (2009) 805–808

Scripta MATERIALIA

www.elsevier.com/locate/scriptamat

High damping capacity in a wide ambient-temperature range in hydrogen-doped and hydrogen-free Ti–45Pd–5Cr martensitic alloy

Y. Zhou,[a,b,c] G. Fan,[a,b] D. Xue,[a,b,c] X. Ding,[a,b] K. Otsuka,[c,a] J. Sun[b,a] and X. Ren[c,a,*]

[a] *Multi-disciplinary Materials Research Center, Xi'an Jiaotong University, Xi'an 710049, China*
[b] *State Key Laboratory for Mechanical Behavior of Materials, Xi'an Jiaotong University, Xi'an 710049, China*
[c] *Ferroic Physics Group, National Institute for Materials Science, Tsukuba 305-0047, Ibaraki, Japan*

Received 8 May 2009; revised 12 June 2009; accepted 30 June 2009
Available online 4 July 2009

Alloys exhibiting high damping capacity in ambient-temperature range (250–400 K) are rare. Here it is reported that a martensitic alloy Ti–45Pd–5Cr shows twin-boundary-related high damping capacity over this temperature range. In the hydrogen-doped martensitic state, a relaxation-type high damping peak ($Q^{-1} \approx 0.09$) exists, extending over 305–370 K. In the hydrogen-free martensitic state, there is a fascinating high-damping plateau ($Q^{-1} \approx 0.05$) over 250–450 K. This work provides new insight into how to develop high damping alloys for the desired temperature range.

Keywords: Ambient temperature; Relaxation; Damping; Twin boundary; Hydrogen

High damping alloys are of significant importance in modern world, as they can suppress noise and reduce mechanical vibrations while having good mechanical strength and ductility [1]. For most practical applications, high damping capacity is required for the wide ambient-temperature range of 250–400 K, which encompasses a range from cold winter temperatures to hot temperatures in a car engine. So far, however, no damping alloy exists that can exhibit high damping capacity over the entire ambient-temperature range. Most high damping alloys exhibit high damping capacity at either low or high temperatures, unable to cover the entire ambient-temperature range [2–5].

Ti–Ni-based martensitic alloys are considered promising as high damping alloys, and their damping behavior has been extensively studied [1,6–14]. In these alloys, two types of damping peaks can be observed. One is associated with martensitic transformation, which strongly depends on the cooling/heating rate, and the peak diminishes at constant temperatures [15]. This transient nature and the temperature hysteresis render the transformation damping peak unusable for applications, although it may appear around room temperature (335 K for TiNi alloy). The other peak is a stable, relaxation-type damping peak, which appears in the martensitic state. It is independent of the cooling/heating rate and is nearly hysteresis free. Such important characteristics have made this relaxation-type damping peak useful for practical applications and thus have drawn keen attention recently [16–23].

The relaxation-type damping peak was found in many Ti–Ni-based alloys such as TiNi and TiNiCu. Recent studies have shown that hydrogen plays an important role in its occurrence [17–21], and it becomes clear now that the interaction between twin boundaries and hydrogen (hereafter abbreviated to "twin boundary–H" interaction) is responsible for appearance of the relaxation peak [22,23]. The interaction of hydrogen atoms with the twin boundaries results in a viscous motion of twin boundaries under AC mechanical stress, and this gives rise to a damping peak associated with the twin boundary–H interaction. Although the damping capacity of such a relaxation-type peak in Ti–Ni-based alloys can be as high as 0.04–0.2, it locates at too low a temperature (200–260 K) to be useful for ambient-temperature (250–400 K) applications.

The present study succeeded in shifting the relaxation-type high damping peak to the useful ambient-temperature range by selecting a martensitic alloy Ti–45Pd–5Cr which exhibits a high martensitic transformation temperature ($M_s \approx 520$ K). It was found that the

---

[*] Corresponding author. Address: Ferroic Physics Group, National Institute for Materials Science, 1-2-1 Sengen, Tsukuba 305-0047, Ibaraki, Japan; e-mail: REN.xiaobing@nims.go.jp

1359-6462/$ - see front matter © 2009 Acta Materialia Inc. Published by Elsevier Ltd. All rights reserved.
doi:10.1016/j.scriptamat.2009.06.033

hydrogen-doped martensitic alloy indeed shows a broad relaxation peak with high damping capacity ($Q^{-1} \approx 0.09$) over a wide ambient-temperature range of 305–370 K. Furthermore, the hydrogen-free martensitic alloy exhibits a temperature- and frequency-insensitive high-damping plateau, which is of a significant level ($Q^{-1} \approx 0.05$) spanning a wide temperature range of 250–450 K, covering the whole ambient-temperature range. The high damping peak and the high damping plateau in the ambient-temperature range suggest that the present martensitic alloy may be a promising candidate for practical applications, and it sheds new light on how to develop new damping alloys for ambient-temperature applications.

A base ingot of Ti–45Pd–5Cr alloy was made by induction melting of 99.9% pure Ti, 99.9% pure Pd and 99.9% pure Cr in an argon atmosphere. The specimens were spark-cut from the base ingot and then solution-treated at 1373 K for 1 h in an evacuated quartz tube, followed by water quenching. Two types of specimen were employed in the present work: one was an H-doped specimen; the other was a H-free specimen. The H-doped specimen was obtained by annealing the solution-treated specimen at 873 K for 4 h in a hydrogen atmosphere. Analysis of the hydrogen content in the specimen was carried out by a thermal conductimetric method after fusion in a current of inert gas. The hydrogen content in the H-doped specimen was ~0.35 at.%. The H-free specimen was prepared by a "dehydrogenation treatment" of the H-doped specimen in a vacuum furnace at 1173 K (see Ref. [22] for method details). The damping behavior of both H-free and H-doped specimen was characterized by a dynamical mechanical analyzer (DMA) of type Q800 from TA Instruments. Bar-shaped specimens of size $4.3 \times 1.35 \times 0.95$ mm^3 were measured in a single cantilever mode under a constant displacement amplitude of 15 μm (the corresponding strain amplitude is 1.7×10^{-3}). The elastic modulus and internal friction as a function of temperature were measured with a multi-frequency (0.2/0.4/1/4/10/20 Hz) mode at a cooling and heating rate of 2 K min^{-1}. To understand the mechanism of the observed damping peak in Ti–45Pd–5Cr alloy, H-free and H-doped TiNi and Ti–30Ni–20Cu specimens were also prepared and measured under the same conditions. These latter two alloys have been known to exhibit a high damping peak due to twin boundary–H interaction.

First, differential scanning calorimetry (DSC) and in situ X-ray diffraction (XRD) measurements were carried out to check the transformation behavior and the crystal structures, respectively (Fig. 1). The exothermic and endothermic peaks on the cooling and heating processes of the DSC curves in Figure 1a show that the specimen undergoes a martensitic transformation at $M_s \approx 520$ K. The XRD profiles at 553 K (Fig. 1b1) and 298 K (Fig. 1b2) indicate that it is a B2–B19 transformation, being the same as the binary Ti–Pd alloys.

The internal friction and elastic modulus of H-doped Ti–45Pd–5Cr alloy as a function of temperature are shown in Figure 2a. Two significant damping peaks are observed in the internal friction curve. The first peak locates at the high-temperature side (peaking at 500 K and vanishing at ~520 K), and is accompanied by a dip in elastic modulus. The peak position does not change with increasing frequency, but the peak height decreases. Clearly, this peak corresponds to the B2–B19 martensitic transformation of this alloy, as indicated by the DSC curve in Figure 1a. Being the same as the martensitic transformation peak of other alloys, this damping peak is transient and vanishes at a constant temperature.

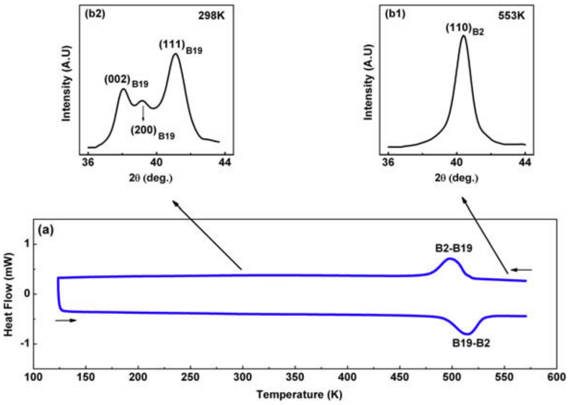

Figure 1. (a) DSC profiles; in situ XRD profiles at (b1) 553 K and (b2) 298 K for Ti–45Pd–5Cr alloy. B2–B19 martensitic transformation with $M_s \approx 520$ K is identified.

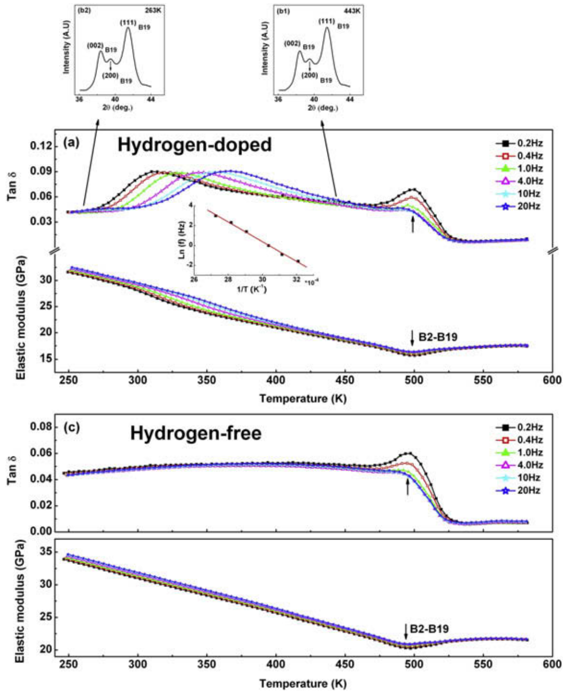

Figure 2. (a) Internal friction and elastic modulus of H-doped Ti–45Pd–5Cr alloy. The in situ XRD measurement at (b1) 443 K and (b2) 263 K shows the same B19 structure above and below the broad peak temperature; thus the broad peak is not associated with a phase transition. The inset in (a) shows that the ln(f) vs. $1/T$ plot of the broad peak fits the Arrhenius law well, indicating that this is a relaxation-type damping peak. The obtained activation energy E and limit relaxation time τ_0 are 0.85 eV and 10^{-13} s, respectively. (c) Internal friction and elastic modulus of H-free Ti–45Pd–5Cr alloy. The relaxation-type damping peak disappears after hydrogen is removed. A temperature-insensitive and frequency-insensitive high-damping plateau is observed.

The second peak, located at the low-temperature side, is most interesting. This damping peak not only has a damping capacity as high as 0.09, but also locates favorably around the ambient-temperature range (305–370 K). This high damping capacity over the wide ambient-temperature range is rare for known high-damping alloys. The invariance in the XRD profile above (Fig. 2b1) and below (Fig. 2b2) the peak temperature shows that there is no structural change over this temperature range; this is consistent with the fact that the elastic modulus does not show a dip. Thus, the broad peak is not associated with a structural transition. The damping peak and the corresponding elastic modulus show strong frequency dispersion, and the peak temperature shifts to a high temperature with increasing frequency. The peak temperature vs. frequency relation follows the Arrhenius relation (see the inset of Fig. 2a), suggesting that this damping peak is of a relaxation type, which bears similar features to the twin boundary–H peak in Ti–Ni-based alloys. The Arrhenius plot yields an activation energy of –0.85 eV and a limit relaxation time of $\sim 10^{-13}$ s. Therefore, the H-doped Ti–45Pd–5Cr alloy shows an ambient-temperature relaxation-type high damping peak in the martensitic state.

Since the H-doped Ti–45Pd–5Cr alloy shows a similar relaxation-type damping peak to that reported in Ti–Ni-based alloys (Refs. [17–23]), it is natural to consider that they have the same origin, i.e., twin boundary–H interaction. To confirm this, the hydrogen was removed from the H-doped Ti–45Pd–5Cr specimen by a dehydrogenation treatment, and then the same DMA measurement was made for the H-free Ti–45Pd–5Cr sample. The result is shown in Figure 2c. The damping peak and the elastic modulus dip corresponding to the B2–B19 martensitic transformation (at ~500 K) still exist, being the same as those of the H-doped specimen. Below the martensitic transformation temperature, however, the relaxation-type damping peak disappears for the H-free specimen. The contrasting results between the H-doped (Fig. 2a) and H-free (Fig. 2c) specimens strongly suggest that the existence of H is indeed a necessary condition for the appearance of the relaxation-type damping peak in Ti–45Pd–5Cr alloy, and supports the twin boundary–H interaction scenario.

In the following, the temperature range and the damping capacity of this relaxation peak are compared with the damping peaks in other damping alloys, as shown in Figure 3. The well-known high-damping alloy Mn–30Cu shows a high damping capacity ($Q^{-1} > 0.04$), but it drops drastically above 300 K [2]. Ti–25Nb–(3O) alloy shows a Snoek-type high damping peak ($Q^{-1} > 0.08$), but the temperature is far above ambient temperature (>480 K) [4]; the Zener relaxation peak (e.g., in CuNi) appears well above the ambient temperature (>500 K) [5]. Therefore, only H-doped Ti–45Pd–5Cr alloy exhibits high damping capacity over the ambient-temperature range. This suggests that it is superior to other damping alloys for ambient-temperature applications.

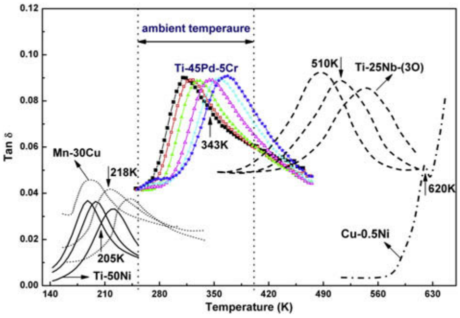

Figure 3. Comparison of the temperature range and damping capacity between the damping peak of Ti–45Pd–5Cr alloy and that of other damping alloys: Mn–30Cu [2], Ti–25Nb–(3O) [4], Cu–0.5Ni [5].

It is of interest to explore why the H-doped Ti–45Pd–5Cr alloy exhibits a twin boundary–H relaxation peak at much higher temperatures (305–370 K) compared with the similar relaxation peak (peaking at 200–260 K) in H-doped Ti–Ni-based alloys. To understand this interesting point, note that the upper temperature limit of the twin boundary–H peak is the martensitic transformation temperature, as it appears only in martensitic state. Therefore, it seems that the twin boundary–H peak temperature is controlled by the corresponding martensitic transformation temperature. The comparison between H-doped Ti–45Pd–5Cr, H-doped TiNi and H-doped Ti–30Ni–20Cu alloys (Fig. 4a) lends support to such a speculation. All these three alloys exhibit a sharp damping peak at the high-temperature side (corresponding to the martensitic transformation) and a broad relaxation-type damping peak at the low-temperature side due to twin boundary–H interaction. Corresponding to the high martensitic transformation temperature of Ti–45Pd–5Cr alloy ($M_s \approx 520$ K), the twin boundary–H peak temperature is also high (305–370 K). However, TiNi and Ti–30Ni–20Cu alloy has much lower M_s temperatures (335 K and 348 K, respectively), and accordingly the twin boundary–H peak temperature is also much lower (200–260 K). Meanwhile,

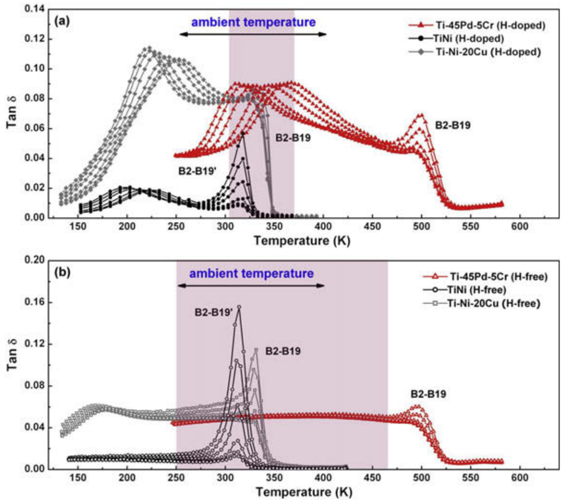

Figure 4. (a) Comparison of the relaxation-type damping peak for H-doped Ti–45Pd–5Cr, H-doped TiNi and H-doped Ti–30Ni–20Cu alloys. (b) Comparison of the high damping plateau for H-free Ti–45Pd–5Cr, H-free TiNi and H-free Ti–30Ni–20Cu alloys. They were tested under the same frequencies: 0.2/0.4/1/4/10/20 Hz. The peak at the high-temperature side of each alloy is the transient peak due to martensitic transformation.

the activation energy obtained by fitting ln(*f*) vs. $1/T$ for Ti–45Pd–5Cr alloy (~0.85 eV) is much higher than that of TiNi (~0.51 eV) and Ti–30Ni–20Cu (~0.67 eV) alloys. Such a correspondence may provide an effective way to obtain high damping capacity in the desired temperature range: selecting an alloy with a suitable martensitic transformation temperature. Nevertheless, further work should be done to understand the quantitative correspondence between the twin boundary–H peak temperature and martensitic transformation temperature.

It should be noted that the H-free Ti–45Pd–5Cr alloy also exhibits interesting damping behavior, as shown in Figure 2c. Although the twin boundary–H peak vanishes in such a situation, the background damping level still maintains a high value of $Q^{-1} \approx 0.05$. This high background damping forms a temperature-insensitive and frequency-insensitive damping plateau, extending from a subzero temperature (250 K) to a high temperature (450 K). This unique high-damping plateau is very important for high damping applications over a wide temperature range and various frequencies.

Figure 4b shows a comparison of the damping plateau in H-free Ti–45Pd–5Cr, H-free TiNi and H-free Ti–30Ni–20Cu alloys. It can be seen that they exhibit a similar damping plateau in their martensitic state, but the upper temperature limit of the plateau is restricted by the martensitic transformation temperature. As a result, the damping plateau of the latter two alloys is restricted to a relatively low temperature range. Therefore, Figure 4b seems to indicate that it is possible to obtain a damping plateau in the desired temperature range by selecting a suitable martensitic transformation temperature. It is quite likely that the damping plateau, which exists in many martensitic alloys, stems from the martensite twin boundaries, as speculated earlier [24–26]; however, it is not clear why twin boundaries result in a damping plateau rather than a peak in the absence of hydrogen. Further work should be done to reveal the origin of this damping plateau. It should be mentioned that, unlike the H-free TiNi and Ti–45Pd–5Cr alloys, which exhibit a “flat” damping plateau in the martensitic state, the H-free Ti–30Ni–20Cu alloy shows a broad “hump” around 180 K, as reported earlier [22]. This hump may be related to a partial B19–B19′ transformation of this alloy [27].

In summary, by doping Ti–45Pd–5Cr alloy with hydrogen, a relaxation-type high damping ($Q^{-1} \approx 0.09$) peak was obtained which extends over a wide ambient-temperature range (305–370 K). Such a relaxation-type damping peak originates from the twin boundary–H interaction, being the same as that of H-doped Ti–Ni-based alloys, but shifting to higher temperatures owing to the higher martensitic transformation temperature. Furthermore, H-free Ti–45Pd–5Cr alloy demonstrates a fascinating damping behavior: a temperature-insensitive and frequency-insensitive high-damping plateau ($Q^{-1} \approx 0.05$) covering the entire ambient-temperature range (250–400 K). These results suggest that Ti–45Pd–5Cr alloy is a promising high damping alloy for ambient-temperature applications. Finally, the present work suggests that it is possible to control the occurrence of high damping capacity for the desired temperature range by selecting an alloy of a suitable martensitic transformation temperature.

The authors gratefully acknowledge the support of National Natural Science Foundation of China (Grant Nos. 50720145101, and 50771079), National Basic Research Program of China under Grant No. 2004CB619303, as well as NCET and 111 project of China. The authors thank S. Ito for the chemical analysis of the specimens.

[1] K. Sugimoto, Membr. Sci. Ind. Res. Osaka Univ. 35 (1978) 31.
[2] F.X. Yin, T. Sakaguchi, Q.C. Tian, A. Sakurai, K. Nagai, Mater. Trans. 46 (2005) 2164.
[3] H. Saitoh, N. Yoshinaga, K. Ushioda, Acta Mater. 52 (2004) 1255.
[4] F.X. Yin, S. Iwasaki, D.H. Ping, K. Nagai, Adv. Mater. 18 (2006) 1541.
[5] B. Ya. Pines, Den Ge-Sen, in: B.N. Finkel’shtein (Ed.), Relaxation Phenomena in Metals and Alloys, Authorized Translation from the Russian, Consultants Bureau: New York, 1963, pp.222–228.
[6] K. Otsuka, C.M. Wayman (Eds.), Shape Memory Materials, Cambridge University Press, Cambridge, 1998.
[7] K. Otsuka, X. Ren, Prog. Mater. Sci. 50 (2005) 511.
[8] I. Yoshida, D. Monma, K. Iino, K. Otsuka, M. Asai, H. Tsuzuki, J. Alloy Compd. 355 (2003) 79.
[9] R. Hasiguti, K. Iwasaki, J. Appl. Phys. 39 (1968) 2182.
[10] K. Iwasaki, R. Hasiguti, Trans. JIM 28 (1987) 363.
[11] I. Yoshida, D. Monma, K. Iino, T. Ono, K. Otsuka, M. Asai, Mater. Sci. Eng. A 370 (1–2) (2004) 444.
[12] J.S. Zhu, R. Schaller, W. Benoit, Phys. Lett. A 141 (1989) 177.
[13] H. Lin, S. Wu, T. Chou, J. Alloy Compd. 355 (2003) 90.
[14] S. Wu, H. Lin, T. Chou, Mater. Trans. 47 (2006) 711.
[15] J. Van Humbeeck, in: Mechanical Spectroscopy Q^{-1}, TransTech, Zurich, 2001, p. 382.
[16] J. San Juan, M.L. Nó, J. Alloys Compd. 355 (2003) 65.
[17] A. Biscarini, B. Coluzzi, G. Mazzolai, F.M. Mazzolai, A. Tuissi, J. Alloys Compd. 356–357 (2003) 669.
[18] F.M. Mazzolai, B. Coluzzi, G. Mazzolai, A. Biscarini, Appl. Phys. Lett. 85 (2004) 2756.
[19] T. Sakaguchi, T. Uehara, Y. Kogo, S. Takeuchi, N. Igata, Mater. Trans. 46 (2005) 1306.
[20] B. Coluzzi, A. Biscarini, G. Mazzolai, F.M. Mazzolai, A. Tuissi, E. Villa, Key Eng. Mater. 319 (2006) 1.
[21] F.M. Mazzolai, A. Biscarini, B. Coluzzi, G. Mazzolai, E. Villa, A. Tuissi, Acta Mater. 55 (2007) 4243.
[22] G. Fan, Y. Zhou, K. Otsuka, X. Ren, K. Nakamura, T. Ohba, T. Suzuki, I. Yoshida, F. Yin, Acta Mater. 54 (2006) 5221.
[23] G. Fan, Y. Zhou, K. Otsuka, X. Ren, Appl. Phys. Lett. 89 (2006) 161902.
[24] J. Van Humbeeck, in: T.S. Ke (Ed.), Proceedings of ICIFUAS-9, Pergamon Press, New York, 1989, p. 337.
[25] J. Van Humbeeck, in: Proceedings of ICIFUAS-96, J. de Physique IV, Colloque C8, Suppl. J. de Phys. III6, 1996, p.371.
[26] J. Van Humbeeck, Mat. Sci. Forum 382 (2001) 366.
[27] H. Miyamoto, T. Taniwaki, T. Ohba, K. Otsuka, S. Nishigori, K. Kato, Scripta Mater. 53 (2005) 171.